RSC Advances

ROYAL SOCIETY OF CHEMISTRY

www.rsc.org/advances

The Electrochemical Behaviors of Tetrahydropalmatine at Nickel Nanoparticles/Sulfonated Graphene Sheets Modified Glassy Carbon Electrode

Haihang Wang,[a] Haiyun Zhai,*[a] Zuanguang Chen,[b] Zhixian Liang,[a] Shumei Wang,[ac] Qing Zhou,[a] Yufang Pan[a]

[a]College of Pharmacy, Guangdong Pharmaceutical University, Guangzhou 510006, China.

E-mail: zhaihaiyun@126.com Fax: +86-20-3935-2129.

[b]School of Pharmaceutical Science, Sun Yat-sen University, Guangzhou 510006, China.

[c]The Key Unit of Chinese Medicine Digitalization Quality Evaluation of SATCM, State Administration of TCM, Guangzhou 510006, Guangdong, China.

Abstract

A novel electrochemical sensor was designed to determine tetrahydropalmatine (THP) by using nickel nanoparticles deposited on sulfonated graphene sheets-modified glassy carbon electrode (NiNPs/SGS/GCE). The components and morphological properties of NiNPs/SGS nanocomposites were investigated by scanning electron microscopy. The anodic peak current (Ipa) of THP at GCE modified with NiNPs/SGS was much higher than those at the bare GCE and SGS/GCE due to the enhance effect of the modified nanomaterials. Differential pulse voltammetry (DPV) disclosed a good linear relationship between Ipa and concentrations of THP (0.50-20.0 μM), with the limit detection of 0.17 μM. Finally, the modified electrode was successfully applied for the determination of THP in Yuanhu Zhitong capsules.

Keywords: sulfonated graphene, nickel nanoparticles, tetrahydropalmatine, modified electrode

1. Introduction

Traditional Chinese medicine has played an important role in the prevention and treatment of diseases in China for thousands of years. Over centuries, the preparations of Yuanhu, as traditional Chinese medicine, have been widely used[1] to alleviate spasticity, abdominal and menstrual pains,[2, 3] and increasingly studied nowadays for the pharmacologic effects on dementia and hepatotoxicity. [4-7] In addition, *rhizoma corydalis* has been successfully formulated into tablets, capsules, injections and

liniments. Of these traditional Chinese medicines, tetrahydropalmatine (THP) is the most effective therapeutic constituent. Therefore, determining THP in the presence of other ingredients is important for quality control.

Up to now, a variety of methods have been used to detect THP, including high performance liquid chromatography (HPLC),[8] and some other liquid chromatography (LC) coupled techniques, such as LC-tandem mass spectrometry (LC-MS/MS),[9] LC-electrospray ionization mass spectrometry (LC-ESI-MS),[10] ultra performance liquid chromatography with fluorescence detection (UPLC-FLD),[11]LC-triple quadrupole tandem mass spectrometry (UPLC-QTOF-MS/MS)[12] and ultra-fast LC with tandem mass spectrometry (UFLC-MS/MS).[13] Compared with these methods, electrochemical method is easily operable, simple, timesaving and highly sensitive. This method is particularly suitable for highly sensitive, rapid analysis of THP in traditional Chinese medicine, which has rarely been reported hitherto. Merely Chen et al. managed to detect THP by using carbon nanotubes (CNTs)-modified glassy carbon electrode (GCE) with square wave voltammetry (SWV). Given the excellent properties of electrochemical sensors, it is worthy of establishing new strategies for electrochemical analysis.

Graphene (GR) is a two-dimensional sheet of sp^2-bonded carbon atoms, which is arranged in a honeycomb lattice perfectly.[14] Owing to extraordinary physical and electrical properties, GR has already shown enormous potentials in a variety of fields including electronics,[15] biomedicine,[16] environment,[17] engineering[18] and sensors.[19] In the electrochemical field, GR can improve the electrocatalytic performance on the surface of modified GCE. At the same time, its unique 2-dimensional plane structure provides a perfect surface for supporting the nanoparticles (NPs) of metal and metal-oxide catalysts.[20] However, GR hardly disperses in water solutions because of high hydrophobicity, which can mainly be attributed to van der Waals bonding and strong π-π conjugation. To improve its dispersibility, GR has been mixed with additives such as surfactants, β-cyclodextrin and Nafion, or modified with some specific groups via physical or chemical functionalization. As a water-soluble unit, $-SO_3^-$ has been introduced to increase the solubility of GR,[21] which satisfactorily detected antibiotics[22] and tryptamine.[23]

In addition, NPs of metals, such as silver, gold and platinum, can enhance the electrochemical properties of GR. After being deposited with AuNPs, GR/GCE[24] has been used to detect ascorbic acid, dopamine and uric acid, showing excellent electrochemical performance. $NiFe_2O_4$/GR nanocomposite,[25] Co_3O_4/GR,[26] molecularly imprinted/nano-Fe_3O_4/SiO_2,[27] AuNPs/GR,[28] and CNTs/GR[29] have been used to modify imprinted electrochemical sensor. Besides, NiNPs have a favorable electrochemical performance too.[30] In this study, a novel GCE electrode modified by GR-nickel was developed and used for the simultaneous detection of ascorbic acid (AA), dopamine (DA) and uric acid (UA). The detection limits attained by differential pulse voltammetry (DPV) were 30 μM, 120 nM and 0.46 μM for AA, DA and UA respectively. Long et al.[31] prepared an imprinted electrochemical sensor based on cobalt-nickel bimetallic nanoparticles by one-step electrodeposition on GR-modified carbon electrode for the sensitive determination of octylphenol. The responsive currents of the imprinted sensor were linearly related with the concentrations from 1.0×10^{-4} to 1.0×10^{-1} μM, with the detection limit of 3.6×10^{-5} μM. The developed sensors provided wider linear ranges and lower limits of detection (LOD) for detecting the components with electrochemical activity compared with those of other previous methods. Expectably, NiNPs can be well deposited at uniquely structured sulfonated graphene sheets (SGS).

In this study, NiNPs-modified SGS hierarchical nanostructure was prepared and used to modify a glassy carbon electrode (NiNPs/SGS/GCE). This modified electrode showed excellent electrochemical properties against THP. Cyclic voltammetry (CV) and DPV were used to evaluate the electrochemical behavior of THP under the optimum conditions at NiNPs/SGS/GCE. The anodic currents of THP at the electrode significantly increased. Particularly, the modified electrode showed much stronger electrochemical responses toward THP in samples than other working electrodes did. This method is

easily operable, simple, timesaving as well as highly stable and sensitive, with low detection limit of THP.

2. Experiment

2.1. Reagents and apparatus

THP was obtained from Aladdin Reagent Co, Ltd. (Shanghai, China). Graphite powder (99%, 40 nm) and hydrazine (98 wt% in water) used for synthesizing GO and SGS were gained from Aladdin Reagent Co, Ltd. (Shanghai, China). The phosphate buffer solutions (PBS) with pH ranging from 3.0 to 10.0 were prepared by mixing stock solutions of 0.2 M $NaH_2PO_4$and 0.2 M Na_2HPO_4, and pH was adjusted with NaOH (1.0 M) and H_3PO_4 (1.0 M) solutions. Unless otherwise stated, all the other chemicals were of analytical grade and purchased from Guangzhou Chemical Reagent Co. Ltd. (Guangzhou, China). THP standard solution (1.0×10^{-3} M) were prepared in deionized water daily. All the aqueous solutions were configured by deionized water.

All the electrochemical determinations such as CV, DPV and Chronocoulometry (CC) were performed on a CHI 850C electrochemical workstation (CH Instrument, Austin, Texas, USA) with a conventional three-electrode system. Bare or modified GCE (Φ = 3.0 mm) acted as the working electrode, a platinum electrode was used as the auxiliary electrode (Gaoss Union, Wuhan, China) and an Ag/AgCl-saturated 3.0 M KCl electrode was used as the reference electrode respectively. All the electrochemical measurements were operated in N_2-saturated 0.1 M PBS. The surface of the modified electrode was examined by scanning electron microscope (SEM) and energy-dispersive spectrometer (SHIMADZU SSX-550, Japan). Fourier-transform infrared (FT-IR) spectrum was obtained on a Mattson Cygnas 100 FT-IR spectrometer (Shelton, USA). XPS was recorded on an X-ray photoelectron spectroscopy/ESCA (Kratos Axis Ultra DLD, U. K.). Raman was recorded on a Raman spectroscopy (Lab RAM Armis, H. J. Y. , France).

2.2. Preparation of graphene oxide (GO) and SGS

GO was synthesized from graphite powders according to the modified Hummers method.[32] Water-soluble SGS were prepared from GO by the following three steps.[33, 34] Firstly, 75 mg dried GO was dispersed in 75 mL water by sonication for 30 min. After the dispersion was centrifuged at 4000 rpm, a clear and brown dispersion of GO formed. Then, 600 mg sodium borohydride in 15 mL water

was added into the dispersion of GO after pH was adjusted to 9-10 with 5 wt% sodium carbonate solution. The mixture was thereafter heated at 80 °C and kept for 1 h under constant stirring. The resultant product was centrifuged and washed with deionized water several times to obtain partially reduced GO. In the second step, the partially reduced GO was redispersed in 75 mL water through mild sonication. Then, 46 mg sulfanilic acid was dissolved in 5 mL water and the resulting solution was added into 5 mL water containing 18 mg sodium nitrite and 0.5 mL of 1.0 M HCl in ice bath to prepare aryl diazonium salt. The obtained aryl diazonium salt was added into the dispersion of partially reduced GO, with temperature strictly controlled below 5 °C. After the mixture was kept for 2 h under stirring to allow complete reaction, the resulting black suspension was centrifuged, washed with water and redispersed in 75 mL water. In the last step, 2 g hydrazine in 5 g water was added into the dispersion. The mixture was kept at 100 °C for 24 h under stirring to complete the reduction. The homogeneous suspension of SGS was subsequently centrifuged and purified by being washed with water. The prepared SGS were dispersed in water as test solutions of 0.5 mg mL^{-1} by a few minutes of sonication.

In order to characterize GO and SGS, Fig. S1 presents the FT-IR spectrum of GO (Fig. S1a) displays well-defined characteristic peaks at (C–O) = 1066.69 cm^{-1}, (C–C) = 1622.97 cm^{-1} and (C–O) = 1730.77 cm^{-1}. And SGS(Fig. S1b), the (C–O) = 1733 cm^{-1} band disappeared. Moreover, there were peaks at (S–O) = 1120.02 cm^{-1} and (S–O) = 1183.17 cm^{-1}, demonstrating the successful reduction of GO to SGS nanomaterials. And Fig. S2 showed us that the Raman spectra of GO sample is characterized by a D-band at 1300 cm^{-1} and a G-band at 1650 cm^{-1}.[35,36] The G-band originate from in-plane vibrations of sp^2-carbon atoms and is a doubly degenerate phonon mode (E2g symmetry) at the Brillouin zone center, while the D-band (symmetry A1g mode) usually results from the presence of sp^3 carbons or defects on graphene sheet,[37] and renewal of sp^2 carbon on grapheme oxide.[38]

2.3. Preparation of electrode

Before modification, bare GCE (Φ = 3 mm) was brightened with 0.05 μm α-Al_2O_3 until a mirror formed. Afterwards, the polished electrode was douched with deionized water, sonicated in HNO_3 (1:1 v/v), ethanol and deionized water successively, and dried in air at room temperature. Then 10 mg SGS were dissolved in 10 mL deionized water. Thereafter, the dispersion was dispersed equably at GCE with a micro-syringe and the solvent was evaporated at room temperature in air to obtain SGS/GCE. Then, CV scanning was performed at SGS/GCE with a potential of -0.6 to 0.6 V vs. Ag/AgCl at a

scanning rate of 0.05 V s^{-1} in 5.0×10^{-3} mol L^{-1} $Ni(NO_3)_2$containing 0.1 mol L^{-1} KNO_3. The obtained modified electrode was denoted as NiNPs/SGS/GCE.

2.4. Preparation of samples

Yuanhu Zhitong (YZT) capsules were purchased from Longfa Pharmaceutical Co., Ltd. (Batch No. 130601) and pretreated according to a previous literature.[39] Capsule contents (2.0 g) were added into 50 mL methanol and refluxed at 85 °C for 30 min, after which the mixture was filtered and the filtrate was evaporated in water bath at 80 °C. Then, 30 mL of 1 wt% hydrochloric acid was added into the residue. The mixture was filtered and washed with 20 mL ethyl acetate twice. Subsequently, ethyl acetate was collected and washed with 20 mL of 1% (wt%) hydrochloric acid twice. After pH was adjusted to 10-11 by adding 50% sodium hydroxide, the analyte was extracted 5 times with 30 mL diethyl ether-extracted acid water solution. The extracts were mixed, dried in water bath at 95 °C, and diluted to 5 mL with methanol. The sample solution was filtered using a 0.45 μm filter and then pH was adjusted to 6.0 using concentrated NaOH (1.0 M) and H_3PO_4 (1.0 M).

3. Results and discussion

3.1. Characteristics of NiNPs/SGS/GCE

SEM images of surface morphologies (Fig. 1.) show us that there are many irregular folds on the surface of SGS/GCE (Fig. 1A). After electrodeposition, numerous orderly nano-spheroidal particles adhered to the surface of SGS/GCE, with the sizes ranging from 20 nm to 150 nm (Fig. 1B).

In order to further confirm the composition of the deposited nanoparticles, the morphology of NiNPs/SGS/GCE was examined by using energy-dispersive spectrometer that showed the existence of Ni (Fig. 1C). A peak at 1.74 keV and 3.73 keV can be assigned to Nickel. The sample was further studied by XPS and the result relevant to the investigation was shown in Fig. 1D. It could be seen that the peaks of Ni and Sulfur (S), and at 853.5 eV and 872.1 eV corresponded to Ni $2p_{3/2}$ and Ni $2p_{1/2}$[40] from Fig. S3A, the peaks at 161.4 eV and 170.4 eV corresponded to S(VI) $2p_{3/2}$ and S(VI) $2p_{1/2}$[41] from Fig. S3B. And the two peaks at 851.2 eV and 874.3 eV corresponded to Ni(II) $2p_{3/2}$ and Ni(II) $2p_{1/2}$, after peak coupling the content of Ni(II) is very lower than NiNPs with a ratio of 1:8. The existence of Ni(II) was probably due to the oxidation of NiNPs. We could infer that the CV scanning with a potential of -0.6 to 0.6 V vs. Ag/AgCl at the scanning rate of 0.05 V s^{-1} in 5.0×10^{-3} mol L^{-1} $Ni(NO_3)_2$ containing 0.1 mol L^{-1} KNO_3 could deposit NiNPs successfully.

The effective surface area of NiNPs/SGS/GCE was calculated by performing CV according to the Randles-Sevcik equation (Eq. (1)):[42]

$$Ipa(\mu A) = 2.69\times10^{5}\, n^{3/2} A_{eff} D^{1/2} v^{1/2} c \quad (1)$$

Where Ipa represents the peak current, n represents the number of electrons transferred, A_{eff} represents the electroactive area (cm^2), D represents the diffusion coefficient of 5.0 mM $K_3Fe(CN)_6$ and 0.1 M KCl ($cm^2\ s^{-1}$), v represents the scan rate ($V\ s^{-1}$) and c is the bulk concentration of the sensor ($mol\ cm^{-3}$). As a result, the surface area of bare GCE, SGS/NiNPs, NiNPs/SGS/GCE were calculated as 5.16 mm^2, 6.23 mm^2, 6.76 mm^2 at a scan rate of 0.05 $V\ s^{-1}$(n=1, $D=7.6\times10^{-6}\ cm^2\ s^{-1}$),[43] the surface area of NiNPs/SGS/GCE was higher than those of bare GCE and SGS/GCE, indicating that SGS and NiNPs greatly enlarged such area of GCE and exerted a promote effect on the electrocatalytic activity of the sensor.

Preferred position for Fig. 1.

3.2. Electrochemical behaviors of THP at different electrodes

The electrochemical activities of bare GCE (Fig. 2A(a)), NiNPs/GCE (Fig. 2A(b)), SGS/GCE (Fig. 2A(c)) and NiNPs/SGS/GCE (Fig. 2A(d)) against 10.0μM THP in PBS (pH 6.0) were investigated by cyclic voltammograms (CVs) bubbled with nitrogen. CVs were recorded in the potential range of 0.3 to 1.2 V. There was a weak signal for THP at the bare GCE, but the anodic peak current (Ipa) evidently increased after SGS were dispersed or NiNPs were deposited. When NiNPs were deposited on SGS/GCE, Ipa of THP was further enhanced from 24.7 μA to 30.1 μA. The enhanced signals may be ascribed to the remarkable promote effect of NiNPs and SGS, which was favorable to the irreversible electrochemical oxidation reaction. Therefore, the NiNPs/SGS-modified electrode may be a proper sensor for THP. While the electrochemical activities of bare GCE (Fig. 2B(a)), SGS/GCE (Fig. 2B(b)), NiNPs/SGS/GCE (Fig. 2B(c)) against 0 M THP in PBS (pH 6.0) at the same atmosphere.

Preferred position for Fig. 2.

3.3. Optimization of experimental conditions

3.3.1. Effect of modified quantity of SGS

The influence of amount of SGS suspension on the electrochemistry behavior of 10.0 μM THP was investigated in 0.1 M PBS (pH 6.0), as shown in Fig. 3A. *Ipa* of THP increased significantly with

rising amount of SGS suspension from 4.0 to 10.0 μL at which *Ipa* reached maximum, while the diffusion coefficient increased from 1.19×10^{-6} cm^2 s^{-1} to 1.36×10^{-6} cm^2 s^{-1}. When the suspension amount exceeded 10.0 μL, the peak signal weakened to approximately 1.31×10^{-6} cm^2 s^{-1} with the suspension amount range from 12.0 μL to 14.0 μL. The influence may be related to the thickness of the film formed by SGS.[44] Over thickness probably weakened the plane structure of SGS and reduced the electrical conductivity. Therefore, 10.0 μL of SGS was used in the following experiment.

Preferred position for Fig. 3.

3.3.2. Effect of deposition time on the SGS-modified electrode

In the experiment, NiNPs were electrodeposited by CV. To a large extent, the distribution of NiNPs influenced the electrochemical conductivity and electron transfer, depending on the setting number of deposition segments. As shown in Fig. 3B, *Ipa* of THP is dramatically augmented after electrodeposition of NiNPs. The potential range was chosen as 0.3 V to 1.2 V. In addition, the peak current, which rose with increasing deposition time less than 200 s, slightly decreased at over 200 s. Therefore, 200 s was selected as the optimum deposition time.

3.3.3. Effect of pH

The mechanism by which THP was electro-oxidized at NiNPs/SGS/GCE was postulated by analyzing the relationship between anodic peak potentials (Epa) and pH. The effect of pH on the electrochemical response of THP at NiNPs/SGS/GCE was investigated by CVs at pH from 3.0 to 10.0 (Fig. 4A). Ipa gradually increased with rising pH from 3.0 to 6.0 at the scan rate of 0.05 V s^{-1}, and reached maximum at pH 6.0 (Fig. 4B). When pH exceeded 6.0, the current dropped with increasing pH. Considering the sensitivity for the determination of THP, pH 6.0 was chosen for subsequent analytical experiments. Furthermore, Epa of THP shifted towards the negative direction with increasing pH, suggesting that protons were directly involved in the oxidation. The relationship between Epa and pH followed a linear regression equation of Epa (V) = -0.0390pH+0.990 (r = 0.9953) (Fig. 4B). According to the Nernst equation (Eq. (2)).

$aOx + ne^- \rightarrow bRed$

$$\varphi(\mathrm{Ox/Red}) = \varphi^{\theta}\ (\mathrm{Ox/Red}) + \frac{RT}{nF}\ln\frac{[c(\mathrm{Ox})/c^{\theta}]^{a}}{[c(\mathrm{Red})/c^{\theta}]^{b}} \qquad (2)$$

Where R and F have their conventional meanings, when the temperature is 25 °C, a slope of 0.0390 (approximately 0.0592/2) indicates that the proportion of electrons to protons involved in the reactions was calculated as approximately 2:1 in the electro-oxidation of THP.

Preferred position for Fig. 4.

3.4. Effect of scan rates.

CVs of THP (10 μM) at NiNPs/SGS/GCE were determined at different scan rates (Fig. 5A). Scan rate significantly affected THP response at NiNPs/SGS/GCE in N_2-saturated PBS. Fig. 5B shows Epa of THP positively shifts and its Ipa increases with rising scan rate from 0.01 to 0.35 V s^{-1}. The relationship of Ipa versus $v^{1/2}$ can be expressed by Eq. (3), demonstrating the electrode process was diffusion-controlled:[45]

$$Ipa = 157.86v^{1/2} - 13.19(\mathrm{r} = 0.9979) \quad (3)$$

Furthermore, peak potential was linearly related with the logarithm of scan rate from 0.01 to 0.35 V s^{-1} (Fig. 6C), which can be expressed by Eq. (4):

$$Epa = 0.1331\log v + 0.9101(\mathrm{r} = 0.9975) \quad (4)$$

As the scan rate increased, the peak potential shifted to a more positive value. For a diffusion-controlled and irreversible electrode process, the relationship between peak potential and scan rate follows the Laviron's equation.[46] According to the above results; the electron of kinetics of the irreversible reaction can be obtained by Eq. (5):

$$Epa = E^{\theta} + \frac{RT}{\alpha nF}\ln\frac{RTK_s}{\alpha nF} + \frac{RT}{\alpha nF}\ln v \quad (5)$$

Where E^{0} is the formal potential (V), α is the electron transfer coefficient, D is the diffusion coefficient of bulk solution and R, T and F have their conventional meanings. For the electro-oxidation of THP, an irreversible process, the relationship between Epa and v can be defined with 2.303RT/αnF for the slopes of the regression equations, and αn was calculated to be 0.639, which was further verified according to the Bard and Faulkner equation (Eq. (6)):[47]

$$Ep_1 - Ep_2 = \frac{1.15RT}{\alpha F} \quad (\text{or } \frac{30}{\alpha} \text{ at } 25\ ^{o}\mathrm{C}) \quad (6)$$

Ep_1 and Ep_2 are defined as two peak potentials for each ten-fold increase in v. Thus, α was calculated as 0.352. The number of electrons (n) transferred in the electro-oxidation of THP was calculated as 1.815 (approximately 2). Therefore, two electrons were involved in the oxidation of THP. As suggested by the relationship between Epa and pH, there was one proton in the oxidation at the same time. In other words, the molecular mechanism of reaction of THP may involve transfer of one proton and two electrons (Scheme 1: Oxidition mechanism of THP on NiNPs/SGS/GCE).[48,49]

Preferred position for Scheme 1

Furthermore, the surface concentration (Γ) of THP was further obtained from the slope of the linear plot of Ipa versus $v^{1/2}$ (V s^{-1}) in Fig. 6B, according to Eq. (7).

$$Ipa = \frac{n^2 F^2 \Gamma A_{eff} v}{4RT} \quad (7)$$

Where *n* represents the number of electrons involved in reaction, and A_{eff} is the electro-active surface area (5.16 mm^2) by Eq. (1) of the modified electrode. R, T and F have their usual values. Γ for THP was calculated as 2.75×10^{-10} mol cm^{-2}. Given the low Γ value, the reaction at NiNPs/SGS modified electrodes was controlled by diffusion.

Preferred position for Fig. 5.

3.5. Chronocoulometric study

Chronocoulometric study of THP at NiNPs/SGS/GCE was carried out to investigate the diffusion coefficients (*D*) described by the Anson equation[50] (Eq. (8)):

$$Q\ (t) = \frac{2nFA_{eff} cD^{1/2} t^{1/2}}{\pi^{1/2}} + Q_{dl} + Q_{ads} \quad (8)$$

In Eq. (8), n, A_{eff}, *c*, *t* and *F* are formal or have usual values, *Q* represents the peak current (C), *D* is the diffusion coefficient of THP, Q_{dl} is double layer charge which could be eliminated by background subtraction and Q_{ads} is the Faradic charge. In ordinary diffusion conditions, *Q* is approximately linearly related with $t^{1/2}$, and *D* can be calculated from its slope. According to Fig. S4, $Q(t)$=601.69 $t^{1/2}$-87.61, so the *D* of THP was obtained to be 1.36×10^{-6} cm^2 s^{-1}.

3.6. Determination of THP by DPV

Under the optimized conditions mentioned above, the differential pulse voltammetry of 0.50-20.0 μM THP at NiNPs/SGS/GCE were recorded by DPV in PBS (pH 6.0) at applied potentials of 0.3-1.2 V. *Ipa* was linearly proportional to the concentration of THP, with the linear regression equation of *Ipa* (μA) = 0.259 *c* + 0.551 (μM, r = 0.9988) (Fig. 6). LOD for THP with a signal to noise ratio of 3 was 0.17 μM.

Preferred position for Fig. 6.

Compared to other methods (Table 1), electrochemical method was chosen because of the wider linear range, lower LOD, and easier sample processing. Compared with the preliminary research of THP by SWV,[51] THP was satisfactorily determined by DPV using the fabricated NiNPs/SGS/GCE.

Preferred position for Table 1.

3.7. Repeatability, stability and interference

The repeatability, reproducibility and stability of the sensor were measured by DPV under the optimum conditions. THP (10.0 μM) was successively determined on one NiNPs/SGS-modified electrode 5 times. Since the relative standard deviation (RSD) was 3.2 %, NiNPs/SGS/GCE displayed high repeatability. Meanwhile, the stability of this electrode was evaluated through 4 h of continuous operation by amperometric technique. Over 99.1 % of the *Ipa* response was retained. Moreover, five modified electrodes prepared independently managed to determine 10.0 μM THP with RSD of 1.7 %. After the electrodes were kept at room temperature for half a month, Ipa of 10.0 μM THP was still as high as 94.7 %. Thus, the modified electrode was also highly stable.

In addition, the changes of Ipa were measured in the presence of different concentrations of potential interferences. In actual measurement, a variety of foreign substances in real sample may disrupt the determination of THP. Ipa of THP was measured in the presence of some other species, with the potential interferences and resulting data summarized in Table 2. Obviously, 400-fold K^+, Ca^{2+}, Na^+, Cl^-, Fe^{3+}, SO_4^{2-}, Mg^{2+} and NO_3^- as well as 100-fold salvianolicacid, berberine, ursolic acid, fumalic acid and protopine all failed to affect the detection of 5.0 μM THP. However, the peak currents were interfered by ascorbic acid, imperatorin and uric acid at 5.0 μM.

Preferred position for Table 2.

3.8. Real sample analysis

NiNPs/SGS/GCE was used to measure the content of THP in a Chinese patent drug (YZT capsules). The sample was diluted 100-fold with PBS (pH 6.0) and measured by DPV. Each sample was measured in triplicate. The modified electrode had an obvious signal for THP. After the sample was spiked with 10.0, 14.0 and 20.0 μM THP, well defined peak currents were observed. The recoveries of these samples were 95.4 %, 101.1 % and 99.6 % respectively, and RSD was lower than 5%, revealing that the modified electrode satisfactorily determined THP in YZT capsules.

For comparison, THP was also detected by HPLC on an Ecosil EPS-C18 column (250 mm × 4.6 mm, 5 mm particle size) with the mobile phase of acetonitrile-methanol-0.1 % H_3PO_4(30:25:45, v/v) at a flow rate of 1.0 mL min^{-1}. The column thermostat was set at 25 °C, and the detection wavelength was set at 281 nm.[8]The diluted sample was centrifuged three times and the supernatant was filtered using a 0.45 μm filter, according to the requirement of this HPLC method. Although the recoveries for THP with HPLC ranged from 98.0 % to 99.8 %, the electrochemical method was facile, fast, reliable, highly sensitive, selective and reproducible, without considerable solvent consumption, or time-consuming sample pretreatment. Therefore, NiNPs/SGS/GCE, which had high accuracy and recovery, was potentially applicable to real sample determination. According to our experiments, this electrode can be used to measure the contents of THP in some Yuanhu preparations, such as YZT capsule. The analytical data for various samples given in Table 3 were highly correlated the results of HPLC and proposed sensor.

Preferred position for Table 3.

4. Conclusions

In summary, a novel sensor based on NiNPs electrodeposited on the surface of SGS/GCE was fabricated to determine THP under optimum conditions. Compared to the bare GCE and pristine SGS/GCE, the modified electrode displayed satisfactory electrocatalytic property for the oxidation of THP. THP was rapidly detected with this method. Furthermore, the modified electrode presented a good linear relationship for THP from 0.50 μM to 20.0 μM, with LOD of 0.17 μM. Finally, THP in Yuanhu preparations was successfully determined by the modified electrode, with considerable repeatability, stability and sensitivity. The nanostructure may be applicable to immobilization of biomolecules and fabrication of biosensors.

Acknowledgements

The authors gratefully acknowledge financial support from the National Natural Science Foundation of China (NSFC, Grant No. 21005021 and No. 21375152) Guangdong Provincial Science and Technology Project (No. 2013B040402010 and No. 2010B0203106010).

References

1 X. S. Wu, J. Xu, X. M. Zhang, T. J. Zhang and C. Q. Chen, *Chin. Tradit. Herb. Drugs*，2015，45，1081-1095.

2 J. J. Ou, L. Kong, C. S. Pan, X. Y. Su, X. Y. Lei and H. F. Zou, *J. Chromatogr. A*, 2006, 1117, 163-169.

3 Z. H. Cheng, Y. L. Guo, H. Y. Wang and G. Q. Wang, *Anal .Chim.Acta*, 2006, 555, 269-277.

4 L. H. Xu, Z. L .Gu, X. G. Jiang, R. Sheng, X. Q. Wang and M. L. Xie, *Acta Pharm. Sinica*, 2002, 37, 902-903.

5 R. Sheng, Z. L. Gu, H. Jiang and Y. Cao, *Chin. Tradit. Herb. Drugs*, 2003, 34, 543-545.

6 K. H. Janbaz, S. A. Saeed and A. H. Gilani, *Pharmacol. Res.*, 1998, 38, 215-219.

7 H. L. Wei and G. T. Li, *Acta Pharm. Sinica*, 1997, 32, 331-336.

8 P. Avouris and C. Dimitrakopoulos, *Mater. Today*, 2012, 15, 86-97.

9 C. Wang, S. Li, Y. J. Tang, S. W. Wang, Y. L. Zhang, G. R. Fan, L. Q. Li and Y. Zhang, *J. Pharmaceut. Biomed.*, 2012, 64-65, 1-7.

10 H. D. Ma, Y. J. Wang, T. Guo, Z. G. He, X. Y. Chang and X. H. Pu, *J. Pharmaceut. Biomed.*, 2009, 49, 440-446.

11 M. M. Yu, E. H. Hazem, I. Ahmed, S. B. Kenneth, L. K. Deanna and J. B. Wang, *J. Chromatogr. B*, 2014, 965, 39-44.

12 Y. Y. Zhang, X. Dong, J. Le, J. Wen, Z. B. Lin, Y. L. Liu, Z. Y. Lou, Y. F. Chai and Z. Y. Hong, *J. Pharm. Biomed.*, 2014, 94, 152-162.

13 X. R. Zhang, J. Guan, H. Y. Zhu and T. T. Niu, *J. Chromatogr. B*, 2014, 971,126-132.

14 D. Q. Tang, X .X .Zheng, X. Chen, D. Z. Yang and Q. Du, *J. Pharm. Biomed. Anal.*, 2014, 4, 96-106.

15 K. S. Bhupendra and H. A. Jong, *Electron. Solid-State. Sci.*, 2013, 89, 177-188.

16 M. P. Neupane, S. J. Lee, J. Y. Kang, I. S. Park, T. S. Bae and M. H. Lee, *Macromol. Chem. Phys.*, 2015, 163, 229-235.

17 V. Štengl, J. Henycha, J. Bludská, P. Ecorchard and M. Kormund, *Ultrason. Sonochem.*, 2015, 24, 65-71.

18 M. Eoin, C. T. Brianna, S. Sepidar and G. W. Gordon, *Polym. Degrad. Stab.*, 2015, 111, 71-77.

19 S. S. Varghese, S. Lonkar, K. K. Singh, S. Swaminathan and A. Abdala, *Sens. Actuators, B-Chem.*, 2015, 218, 160-183.

20 V. K. Prashant, *J. Phys. Chem. Lett.*, 2015, 1, 520-527.

21 M. M. Dinesh, K. Saminathan, M. Selvam, S. R. Srither, V. Rajendran and K. V. I. S. Kaler, *J. Power Sources.*, 2015, 76, 32-38.

22 Y. Kitazono, I. Ihara, G. Yoshida, K. Toyoda and K. Umetsu, *J. Hazard. Mater.*, 2012, 243, 112-116.

23 X. R. Xing, S. Liu, J. H. Yu, W. J. Lian and J. D. Huang, *Biosens. Bioelectron.*, 2015, 31, 277-283.

24 C. Q. Wang, J. Du, H. W. Wang, C. E. Zou, F. X. Jiang, P. Yang and Y. K. Du, *Sens. Actuators, B-Chem.*, 2014, 204, 302-309.

25 A. Afkhami, H. Khoshsafar, H. Bagheri and T. Madrakian, *Anal. Chim. Acta*, 2014, 831, 50-59.

26 Z. X. Song, Y. J. Zhang, W. Liu, S. Zhang, G. C. Liu, H. Y. Chen and J. S. Qiu, *Electrochim. Acta*, 2013, 112, 120-126.

27 Z. H. Zhang, L. J. Luo, R. Cai and H. J. Chen, *Biosens. Bioelectron.* , 2013, 49, 367-373.

28 S. Wang, Y. Wang, L. H. Zhou, J. X. Li, S. L. Wang and H. L. Liu, *Electrochim. Acta*, 2014, 132, 7-14.

29 B. Q. Yuan, C. Y. Xu, D. H. Deng, Y. Xing, L. Liu, H. Pang and D. J. Zhang, *Electrochim. Acta*, 2013, 88, 708-712.

30 T. E. Mary Nancy and V. AnithaKumary, *Electrochim. Acta*, 2014, 133, 233-240.

31 F. Long, Z. H. Zhang, J. Wang, L. Yan and B.W. Zhou, *Electrochim. Acta*, 2015, 168, 337-345.

32 W. S. Hummers and R. E. Offeman, *J. Am. Chem. Soc.*, 1958, 80, 1339.

33 Y. Si and E. T. Samulski, *Nano Lett.*, 2008, 8, 1679-1682.

34 S. J. Li, J. Z. He, M. J. Zhang, R. X. Zhang, X. L. Lv, S. H. Li and H. Pang, *Electrochim. Acta*, 2013, 102, 58-65.

35 M. A. Pimenta, G. Dresselhaus, M. S. Dresselhaus, L. G. Cancado, A. Jorio and R. Saito, *Phys. Chem.Chem. Phys. ,* 2007, 9, 1276–1290.

36 M. S. Dresselhaus, G. Dresselhaus and M. Hofmann, *Phil. Trans. R. Soc. London, Ser.* A, 2008, 366, 231–236.

37 A. C. Ferrari and J. Robertson, *Phys. Rev. B: Condens.Matter,* 2000, 61, 14095.

38 D. X. Yang, A. Velamakanni, G. Bozoklu, S. Park, M. Stoller, R. D. Piner, S. Stankovich, I. Jung, D. A. Field, C. A. V. Jr. and R. S. Ruoff, *Carbon*, 2009, 47, 145-452.

39 H. Z. Wei, F. Xie, Y. Rao, X. N. Li, H. H. Zhang and H. X. Jin, *Chin. Tradit. Herb. Drugs.* , 2012, 2, 299-302.

40 S. D'. Addato, V. Grillo, S. Altieri, R. Tondi, S. Valeri and S. Frabboni, *J. Phys.: Condens. Matter*, 2011, 23, 175003.

41 S. Yagi, M. Nambu, C. Tsukada, S. Ogawa, G. Kutluk, H. Namatame and M. Taniguchi, *Appl. Surf. Sci.*, 2013, 267, 45–47.

42 A. J. Bard and L. R. Faulkner, *Wiley, New York*, 1980, 226.

43 M. V. Srackelberg, M. Pilgram and V. Toome, *Ber. Bunsen-Ges. Phys. Chem* 1953, 57, 342-350.

44 K. X. Zhang, L.M. Lu, Y. P. Wen, J. K. Xu, X. M. Duan, L. Zhang, D. F. Hu and T. Nie, *Anal. Chim. Acta*, 2013, 787, 50-56.

45 T. T. Zhang, Q. L. Lang, D. P. Yang, L. Li, L. X. Zeng, C. Zheng, T. Li, M. D. Wei and A. H. Liu, *Electrochim. Acta*, 2013, 106, 127-134.

46 E.Laviron, *J. Electroanal. Chem.* , 1974, 52, 355-393.

47 A. J. Bard and L. R. Faulkner, *Wiley, New York*, 2001.

48 H. Okazaki, K. Onishi, Y. Ikefuji and R. Tamura, *J. Chem. Soc., Perkin Trans. 2*, 1990, 2, 1321-1327.

49 M. Okimoto, Y. Takahashi, K. Numata and G. Sasaki, *Heterocycles*, 2005, 36, 371-375.

50 F. C. Anson, *Anal. Chem.*, 1966, 38, 54-57.

51 X. Chen, T. Liu, X. P. Xu and G. N. Chen, *Fujian Anal.& Testing*, 2012, 21, 21-24.

Figure captions:

Fig.1. SEM images of (A) SGS on GCE; (B) NiNPs/SGS on GCE; (C) Energy spectrum analysis of NiNPs/SGS/GCE surface; (D) X-ray photoelectron spectrum of surface materials of the electrode.

Fig.2. (A) CVs of 10.0μM THP at bare GCE (A(a)), Ni/GCE(A(b)), SGS/GCE (A(c)) and NiNPs/SGS/GCE (A(d)) in 0.1 M PBS (pH 6.0) at a scan rate of 0.05 V s^{-1}; (B) CVs of 0μM THP at bare GCE (B(a)), SGS/GCE(B(b)), NiNPs/SGS/GCE(B(c)).

Fig.3. (A)Effect of amount of SGS dispersion on the peak current of10.0μM THP; (B) The relationship between deposition time and peak current.

Fig.4. (A) CVs of 20.0 μM THP in 0.1 M PBS at pH of 3.0-10.0 from right to left. Scan rate: 0.05 V s^{-1}, deposition time: 200s, initial *E*: 0.3 V, final *E*: 1.2 V; (B) Effects of pH on the *Epa* and *Ipa* of 10.0μM THP in PBS (pH3.0-10.0) on NiNPs/SGS/GCE at the scan rate of 0.05 V s^{-1}.

Scheme 1. Oxidition mechanism of THP on NiNPs/SGS/GCE.

Fig.5. (A) CVs of NiNPs/SGS/GCE in N_2-saturated PBS(pH of 6.0) at different scan rates (0.01, 0.02, 0.03, 0.04, 0.05, 0.06, 0.07, 0.08, 0.09, 0.10, 0.12, 0.15, 0.17, 0.20, 0.25, 0.30 and 0.35 V s^{-1}); (B)Linear relationship between square root of scan rates ($v^{1/2}$) and peak currents of THP; (C)Linear relationship between *Epa* and lg*v* of THP.

Fig.6. (A) DPV of THP on NiNPs/SGS/GCE in PBS (pH=6.0, 0.2M) at the concentrations of (0.5, 1.0, 2.0, 5.0, 10.0, 15.0 and 20.0 μM); (B) Linear relationship of steady state currents versus THP concentration.

Table 1. Comparison with other methods for the determination of THP.

Test method	The measuring object	Concentration range (μM)	LOD(μM)	Reference
LC-MS/MS	L-THP	2.81×10^{-4}-2.81	2.81×10^{-4}	9
LC-ESI-MS	THP	2.81×10^{-3}-1.41	2.8×10^{-3}	10
UPLC–FLD	L-THP and cocaine	7.03×10^{-3}-0.70	7.03×10^{-3}	11
LC–QqQ/MS	(+)-THP and (-)-THP	1.41×10^{-2}-70.3	1.41×10^{-2}	12
UFLC-MS/MS	STR and THP	2.81×10^{-2}-14.1	2.81×10^{-2}	13
RP-HPLC	D-THP and L-THP	2.81×10^{1}-8.44×10^{2}	4.2 and 14.1	2
Electrochemical(CNTS/GCE) by SWV	THP	0.8-50	0.3	51
Electrochemical(NiNPs/SGS/GCE) by DPV	THP	0.50-20.0	0.17	This work

Table 2. Effects of various substances on the determination of THP

substance	Content (mM)	Relative error(%)	substance	Content(mM)	Relative error(%)
K^+	2.0	+1.3	Salvianolic acid	0.5	+2.1
Ca^{2+}	2.0	+1.5	Berberine	0.5	+1.7
Na^+	2.0	+1.2	Ursolic acid	0.5	-2.3
Cl^-	2.0	-2.0	Fumalic acid	0.5	+1.9
Fe^{3+}	2.0	+1.6	Protopine	0.5	+2.2
SO_4^{2-}	2.0	-3.1	Ascorbic acid	0.005	+5.9
Mg^{2+}	2.0	+1.9	Imperatorin	0.005	+6.2
NO_3^-	2.0	-3.4	Uric acid	0.005	+6.9

Table 3. Determination of THP in YZT capsules by electrochemical method and HPLC (n=3).

Technique	Original(μM)	Added(μM)	Founded(μM)	Recovery(%)	RSD(%)
	7.0	3.0	9.86	95.4	1.5
This work	7.0	7.0	14.08	101.1	1.7
	7.0	13.0	19.95	99.6	1.3
	7.0	3.0	9.94	98.0	1.3
HPLC	7.0	7.0	13.89	98.4	1.6
	7.0	13.0	19.97	99.8	1.4

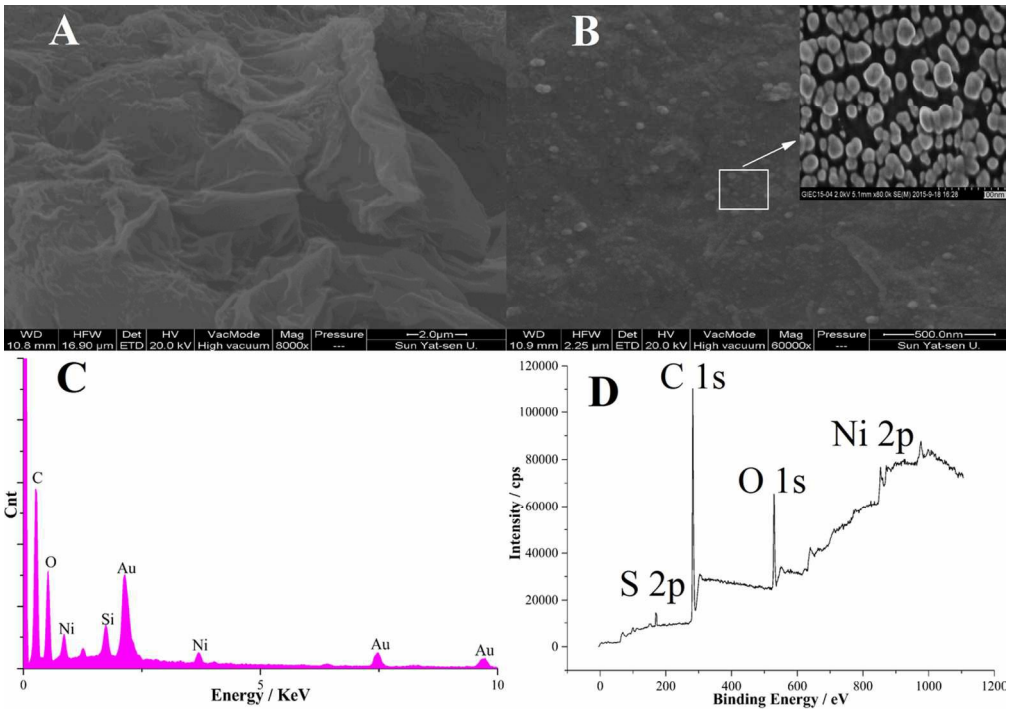

Fig.1.SEM images of (A) SGS on GCE; (B)NiNPs/SGS on GCE; (C) Energy spectrum analysis of NiNPs/SGS/GCE surface; (D) X-ray photoelectron spectrum of surface materials of the electrode.

56x39mm (600 x 600 DPI)

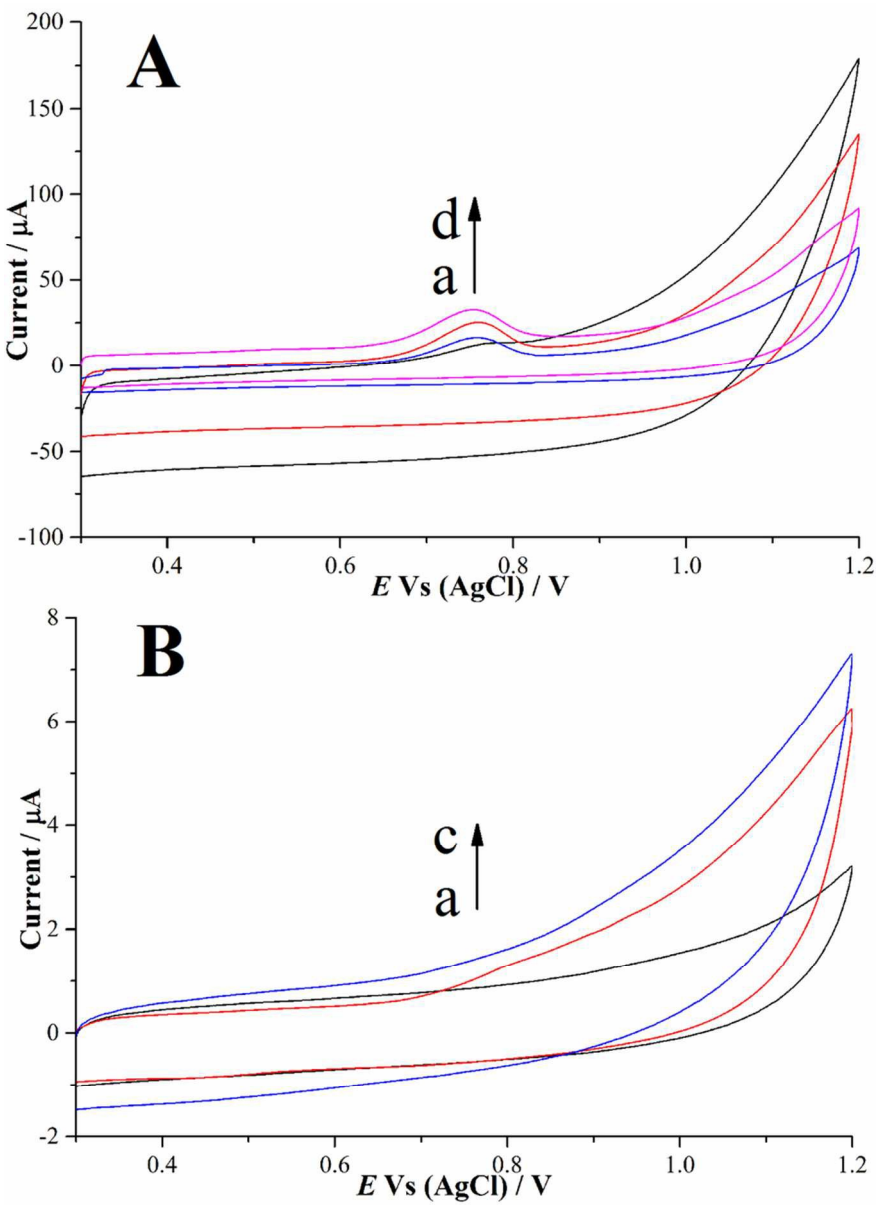

Fig.2. (A) CVs of 10.0μM THP at bare GCE (A(a)), Ni/GCE(A(b)), SGS/GCE (A(c)) and NiNPs/SGS/GCE (A(d)) in 0.1 M PBS (pH 6.0) at a scan rate of 0.05 V s^{-1}; (B) CVs of 0μM THP at bare GCE (B(a)), SGS/GCE(B(b)), NiNPs/SGS/GCE(B(c)).

39x55mm (600 x 600 DPI)

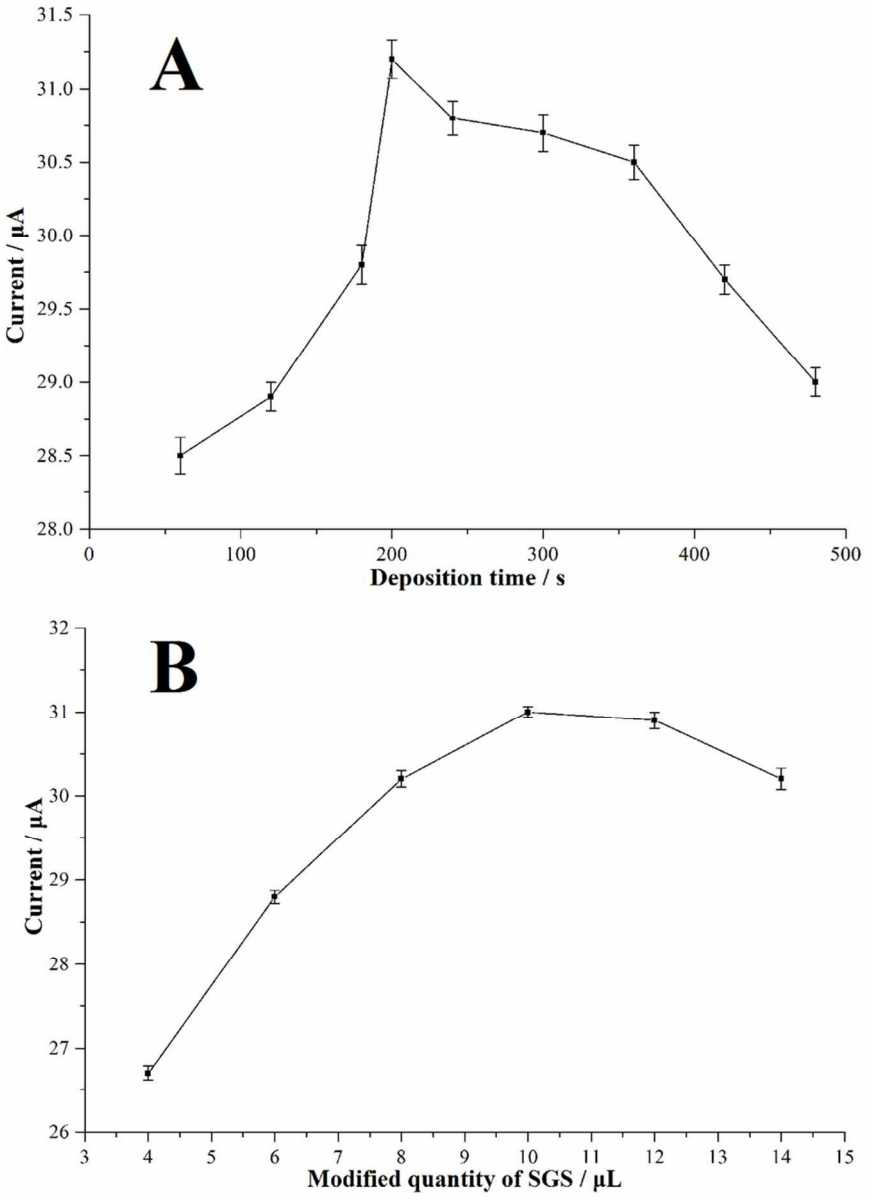

Fig.3. (A)Effect of amount of SGS dispersion on the peak current of10.0 μM THP; (B) The relationship between deposition time and peak current.

39x55mm (600 x 600 DPI)

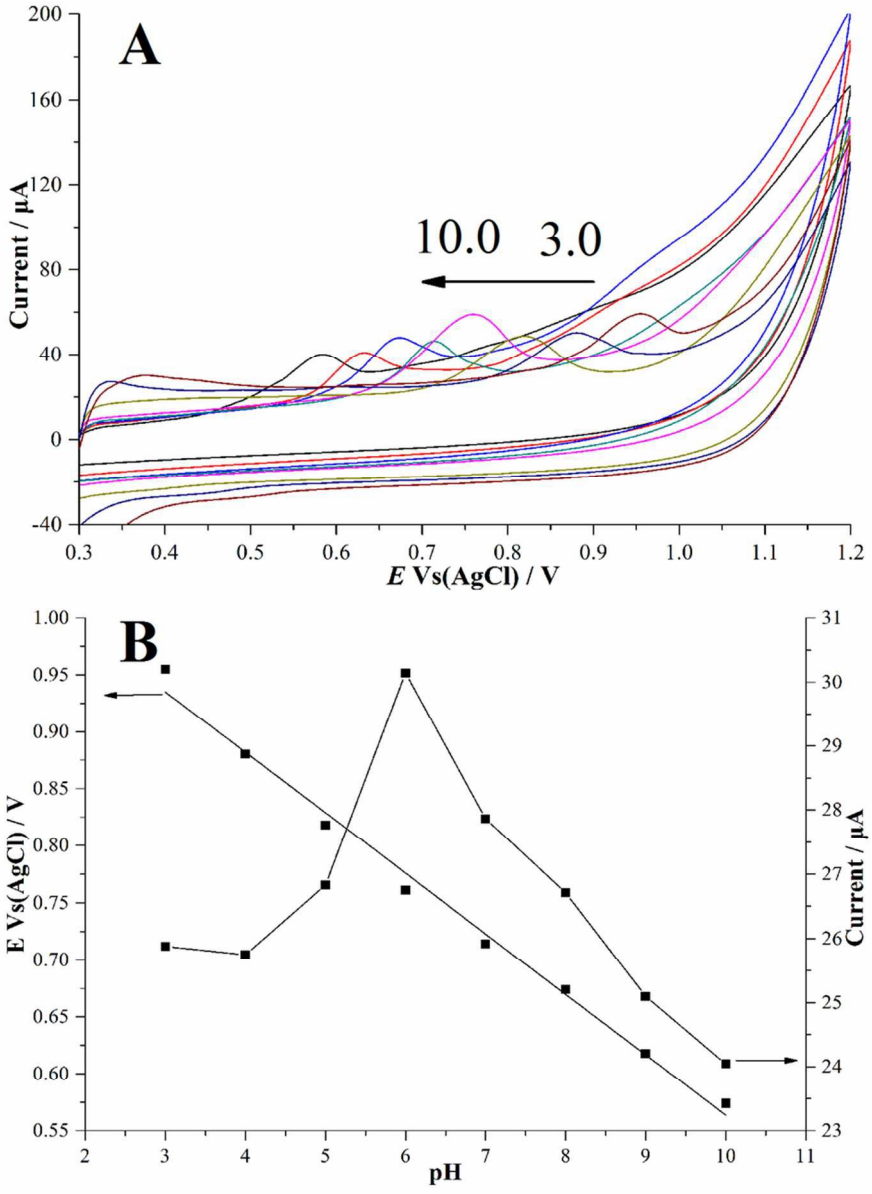

Fig.4. (A) CVs of 20.0 μM THP in 0.1 M PBS at pH of 3.0-10.0 from right to left. Scan rate: 0.05 V s^{-1}, deposition time: 200s, initial E: 0.3 V, final E: 1.2 V; (B) Effects of pH on the Epa and Ipa of 10.0μM THP in PBS (pH3.0-10.0) on NiNPs/SGS/GCE at the scan rate of 0.05 V s^{-1}.

39x55mm (600 x 600 DPI)

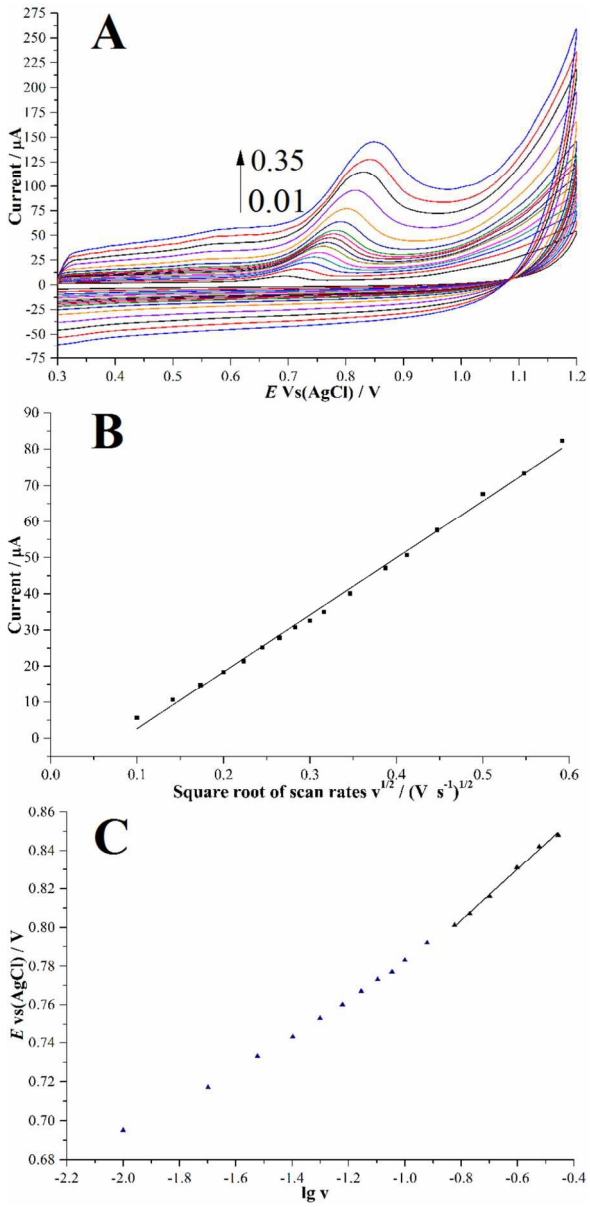

Fig.5. (A) CVs of NiNPs/SGS/GCE in N_2-saturated PBS(pH of 6.0) at different scan rates (0.01, 0.02, 0.03, 0.04, 0.05, 0.06, 0.07, 0.08, 0.09, 0.10, 0.12, 0.15, 0.17, 0.20, 0.25, 0.30 and 0.35 V s^{-1}); (B)Linear relationship between square root of scan rates ($v^{1/2}$) and peak currents of THP; (C)Linear relationship between Epa and lgv of THP.

37x78mm (600 x 600 DPI)

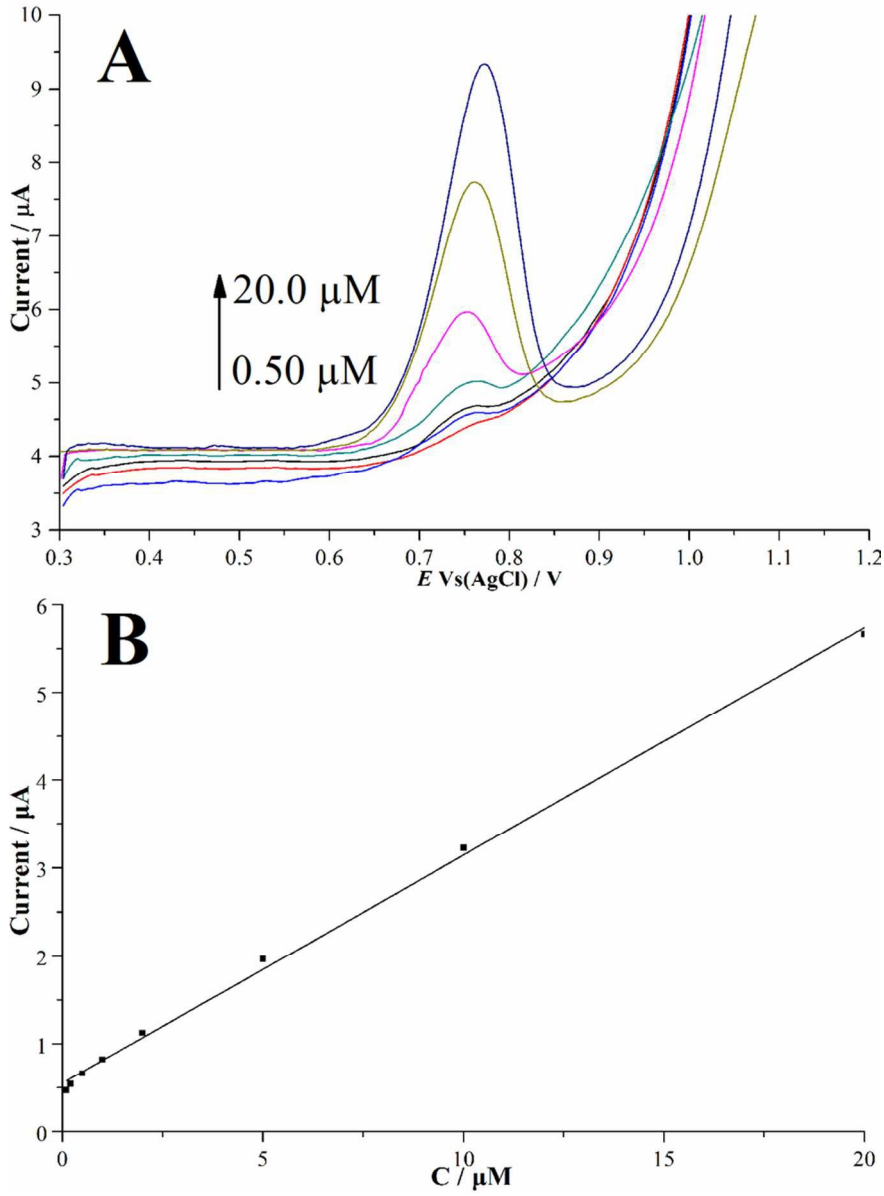

Fig.6. (A) DPV of THP on NiNPs/SGS/GCE in PBS (pH=6.0, 0.2M) at the concentrations of (0.5, 1.0, 2.0, 5.0, 10.0, 15.0 and 20.0 μM); (B) Linear relationship of steady state currents versus THP concentration.

39x55mm (600 x 600 DPI)

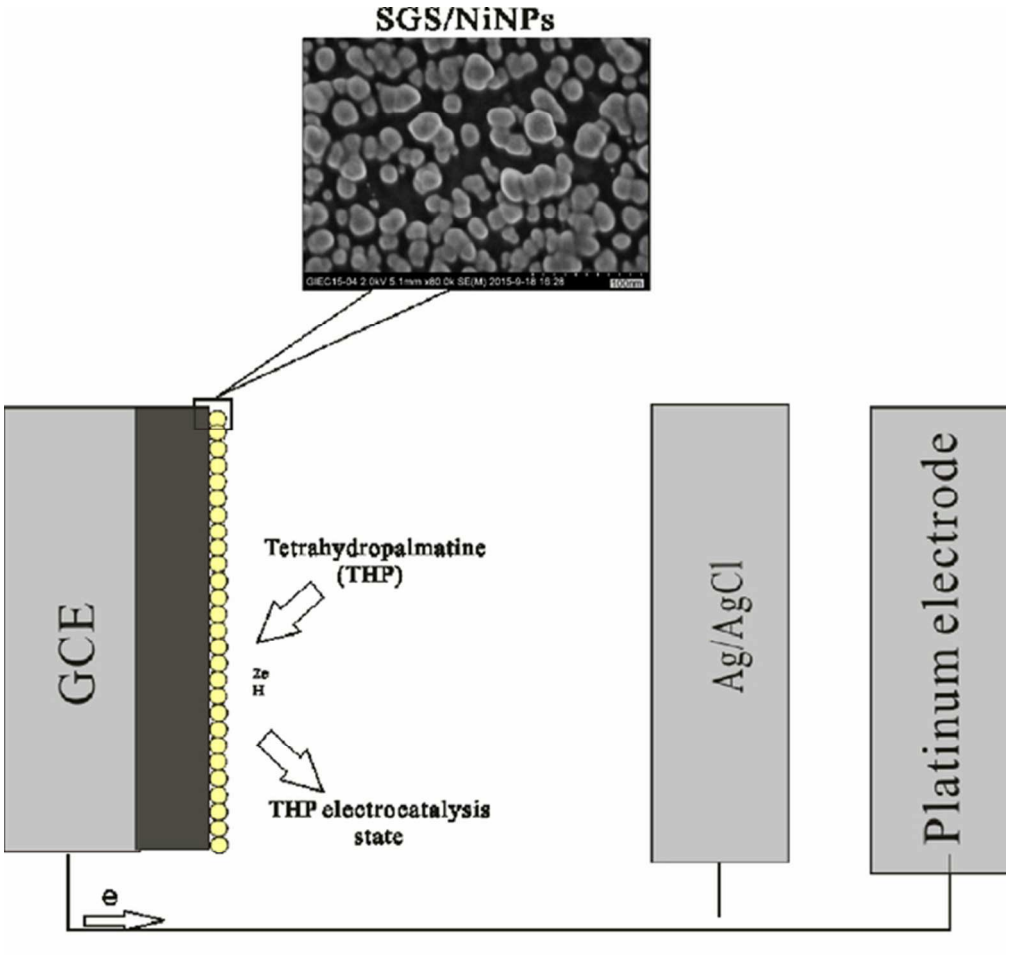

Graphical Abstract

27x26mm (600 x 600 DPI)